An Effort to Fabricate Clinically Relevant Scaffold Using 3D Bioprinting Processes.

Cartwright Nelson, Slesha Tuladhar, and Ahasan Habib

Sustainable Product Design and Architecture Department, Keene State College, Keene, NH 03435, USA.

Abstract

Three-dimensional bio-printing is a rapidly growing field attempting to recreate functional tissues for medical and pharmaceutical purposes. Development of functional tissues and organs requires the ability to achieve large full-scale scaffolds that mimic human organs. It is difficult to achieve large scaffolds that can support themselves without damaging printed cells in the process. The high viscosity needed to support large prints requires high amounts of pressure that diminishes cell viability and proliferation. By working with the rheological, mechanical, and microstructural properties of different compositions, a set of biomaterial compositions was identified to have high structural integrity and shape fidelity without needing a harmful amount of pressure to extrude. Various large scale-scaffolds were fabricated (up to 3.0 cm, 74 layers) using those hybrid hydrogels ensuring geometric fidelity. This effort can ensure to fabricate large scaffolds using 3D bio-printing processes ensuring proper internal and external geometries

Keywords

3D bioprinting, pre-crosslink rheology, printability, large scaffolds, and hybrid hydrogels

1. Introduction

Due to the advancement of 3D bio-printing and bio-compatible materials, the field of tissue engineering and regenerative medicine (TERM) has been growing exponentially in recent years. 3D bio-printing is an innovative technology for fabricating functional tissue, and its growing capabilities along with the increasing availability of compatible materials has helped with its rapid expanse [1]. For attaining the design specific 3D tissue scaffolds, spatial control and repeatability of material deposition are crucial. There are three 3D bio-printing processes such as extrusion-based [2-4], inkjet [5, 6], and laser-assisted [7, 8] bioprinting that achieve these requirements. The extrusionbased bioprinting process has gained comparatively more attraction among them because it is capability of printing a diverse range of materials while allowing higher cell density [9]. Highly porous 3D constructs that serve as a temporary structural support for the growth of isolated cells are often fabricated using naturally growing polymeric materials and hydrogels [10]. Although hydrogels have many benefits such as high water content, biocompatibility, and biodegradability, [11-13], one of the biggest challenges with hydrogels is achieving controlled spatiality of the fabricated 3D scaffold [14]. In order to achieve the desired properties of a particular bio-ink and final structure, different hydrogel materials are mixed to prepare a hybrid hydrogel [15, 16]. Yield strength is one example of a mechanical property that must be correct in order to maintain the dimensional accuracy of the scaffold after the material is extruded from the nozzle [17]. Methods of controlling the yield strength of hydrogel materials include using viscosity modifiers [18-20], changing temperature [21-23], using an external cross-linker [24, 25], incorporating sacrificial materials [26], and controlling intrinsic rheological properties of the hydrogels [27, 28].

Various bi- and tri-valent cations such as $Ca^{2+}[25,29]$, $Ba^{2+}[30]$, $Ga^{3+}[31]$, and $Al^{3+}[32]$ have been used as physical crosslinkers. Among them, $CaCl_2$ and $CaSO_4$ are most common [33]. Pre-crosslinking hydrogels is an approach in which the physical crosslinkers are included when mixing the hydrogel materials before the printing process [34]. In this paper we used both viscosity enhancer and pre-crosslinkers ($CaCl_2$ and $CaSO_4$) to ensure better shape fidelity of hydrogels, improve mechanical properties and achieve a full scaled (in cm scale) printed scaffold. We used alginate and Carboxymethyl Cellulose (CMC) maintaining $\leq 8\%$ solid content as the base hydrogel materials. As pre-crosslinkers, $CaCl_2$ and $CaSO_4$ were used. The effects of the viscosity enhancer and pre-crosslinker were characterized by a set of tests including flow analysis and geometric fidelity tests. Finally, two candidate materials were used to fabricate a large-scale freeform scaffold.

Table 1: (a) Various Composition prepared with different weight percentages of alginate and CMC and (b) An overview of all rheological tests.

	A_xC_y		Pre-crosslinked		D	Rheological tests	Variables	Outcome
<u>:</u>			110 010	ээттке		Steady rate sweep	Shear rate (s ⁻¹): 0.1 to 100	Flow curve, viscosity, shear stress,
2	X	У	0.5% CL	0.5% CS	parameters			shear-thinning behavior
	6	2			Nozzle dia 0.84mm,	Amplitude sweep 3iTT	Shear strain (%): 0.1 to 100	Storage modulus (G') and loss
: `	4	4		(A)				modulus (G"), loss tangent ($\tan \delta$)
. '	4	4	ALC: NO		print speed 20mm/s, pressure 29-45 psi		Time (s)/Shear rate (s-1):	Recovery rate of the hydrogel
	2	6	· /		pressure 29-45 psi		0-60/1, 61-65/100, 66-185/1	
			(a)			***************************************	(b)	·

2. Hybrid hydrogel preparation

A set of hybrid hydrogels were prepared using alginate and carboxymethyl cellulose and all the compositions were pre-crosslinked with CaCl₂ and CaSO₄ respectively. As candidate material, medium (viscosity \geq 2000 cps of 2% in water) viscous Alginate (A) (alginic acid sodium salt from brown algae) and carboxymethyl cellulose (CMC) (pH: 6.80) (Sigma-Aldrich, St. Louis, MO, USA) were used. Alginate is the most commonly biopolymer, composed with (1-4)-linked β-Dmannuronic (M) and α-Lguluronic acids (G). Carboxymethylcellulose (CMC) is an anionic water-soluble biopolymer which is composed with β-D-glucose and β-D-glucopyranose-2-O-(carboxymethyl)-monosodium salt. Both of them are connected via β-1,4-glucosidic bonds [35]. Three hybrid hydrogels composed with various weight percentages of alginate and CMC were pre-crosslinked separately with 0.5% (w/v) calcium chloride (CaCl₂, CL) and 0.5% (w/v) calcium sulphate (CaSO₄, CS) (Sigma-Aldrich, St. Louis, MO, USA) which resulted total six compositions in this paper. We maintained a constant 8% (w/v) solid content of alginate and CMC as shown in Table 1 (a). Food colors are used to differentiate the compositions as shown in Table 1 (a). The extruded filament should demonstrate a consistent surface and constant width which will subsequently create regular grids, square holes, and proper layer height. However, hydrogel with more liquid-like state may fuse the released filament, create circular holes for bi-layer geometry, and eventually close the pore. Therefore, the printability (Pr) [21] of the hydrogel is defined using the following Equation:

$$P_r = \frac{\pi}{4} \frac{1}{C} = \frac{L^2}{16A_a} \tag{1}$$

Where, L and A_a are the perimeter and actual area of the pore. The under gelation (Pr < 1), ideal gelation (Pr = 1), and over gelation (Pr > 1) can be defined using the P_r value. To determine the printability, various scaffolds having 2.5 mm raster width (filament to filament distance) were fabricated with a zig-zag pattern using all compositions. The objective to determining the printability is to identify the shape-holding capacity of the deposited material. Pore closure or the diffusion rate was determined using the equation (2). Pore images were captured using the CK Olympus bright field microscope (Tokyo, Japan) and analyzed using ImageJ software.

$$Diffusion \ rate = \frac{Change \ of \ pore \ area}{Theoritical \ pore \ area} \times 100$$
 (2)

3. Yield and flow stress

Rheological measurements were performed using a rotational rheometer (MCR 102, Anton Paar, Graz, Austria) with parallel plate geometry (25.0 mm flat plate). All measurements were recorded with a 1.0 mm plate-plate gap width at room temperature (25°C). We conducted the rheological measurement at room temperature because our extrusion process was performed at room temperature which also facilitated the quick gelation of the deposited filament [36]. A set of rheological tests such as steady rate sweep test, amplitude test, and three-point interval thixotropic test were done. An overview of those tests is shown Table 1(b).

We performed an amplitude sweep test with a constant frequency of 1 Hz for all compositions to determine the yield and flow stress as shown in Figure 1 (pre-crosslinked with CaSO₄) and Figure 2 (pre-crosslinked with CaCl₂). This test defines the linear region of the material under a subsequent frequency sweep. The shear stress or deformation amplitude is varied while the frequency is kept constant during the test. Storage modulus (G', solid-like) and loss (G'', liquid-like) modulus were resulted from this experiment that can basically identify the complex modulus ($G^* = G' + iG''$). Figures 1 and 2 demonstrate that the solid-like state dominated the liquid-like state at lower shear rate for all compositions. This phenomenon continued until a certain level where both moduli started getting reduced i.e., permanent deformation of internal bonds. This linear viscoelastic range (LVR) indicates the range at which the extrusion can happen without deforming the internal structure of the sample i.e., suspension, preserves the

sedimentation without permanent deformation. The strain rate at the LVR and corresponding G' which is also known as yield stress is shown in Figure 3(a).

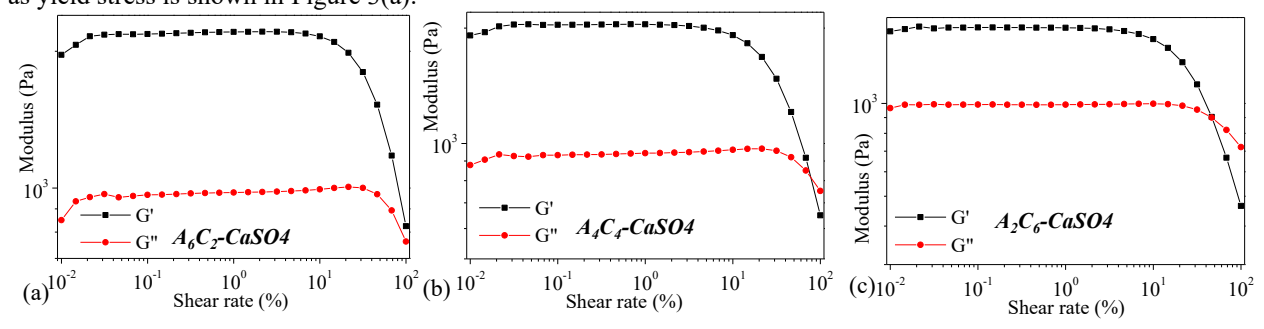


Figure 1: The storage and loss modulus, the linear viscosity range, and gel-point for A₆C₂, A₄C₄, and A₂C₆ compositions pre-crosslinked with 0.5% CaSO₄.

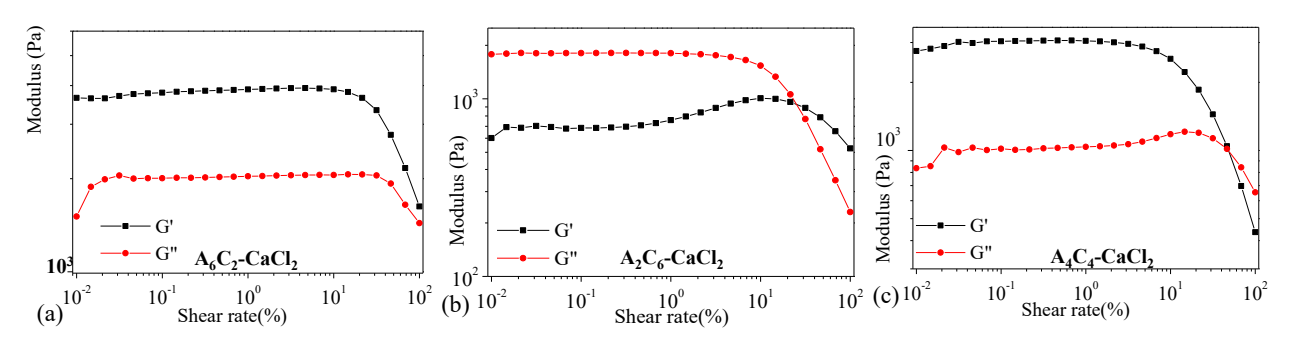


Figure 2: The storage and loss modulus, the linear viscosity range, and gel-point for A₆C₂, A₄C₄, and A₂C₆ compositions pre-crosslinked with 0.5% CaCl₂.

	A_6C_2		A_4C_4		A_2C_6		3	Precrosslinked with CaCl ₂	
	CL	CS	CL	CS	CL	CS	4×10³ -	Precrosslinked with CaSO ₄ -	
% strain at yield point	9.6	16	5	6	4.5	5	€ 3×10³ -	32%	
Yield stress (Pa)	3577	2096	2875	1965	2408	1726	setts 2×10 ³ -	28%	
% of strain at flow point	NA	105	50	80	19	50	i≨ 1×10³ -		
Flow stress (Pa)	NA	679	1105	767	1490	712	(b) 0-		

Figure 3: (a) Yield point, corresponding yield stress, and flow-point, corresponding flow stress for A_6C_2 , A_4C_4 , and A_2C_6 compositions pre-crosslinked with 0.5% CaSO₄ (CS) and CaCl₂ (CL) and (b) Comparison of yield stress FOR A_8C_0 , A_4C_4 , A_2C_6 , AND A_0C_8 compositions pre-crosslinked with 0.5% CaSO₄ and CaCl₂.

It is clear from Figure 3(a) that all compositions pre-crosslinked with CaSO₄ showed comparatively less yield stress than pre-crosslinked with CaCl₂. Due to the molecular structure of CaCl₂, it is readily soluble in water which often leads to an uncontrolled release of Ca²⁺ ion and therefore results more crosslinking rate compared to compositions crosslinked with CaSO₄. Alginate is a negatively charged linear copolymer (M and G blocks) which contains abundance amount of carboxylate ion (-COO-), soluble in the water. The G-block of this material creates bonds to form gels and GM and M blocks increase the flexibility. More number of carboxylate ion (-COO-) facilitates the attraction with Ca²⁺ ion, creates physical bonding, and results higher rate of cross-linking. Therefore, A₆C₂, A₄C₄, and A₂C₆ compositions pre-crosslinked with 0.5% CaCl₂ showed 41%, 32%, and 28% higher yield stress respectively compared to the same compositions pre-crosslinked with 0.5% CaSO₄.

At the LVR region, the storage modulus dictated (G' > G'') for all compositions which indicates a 'gel structure'. There was an intersection point for A_4C_4 and A_2C_6 compositions pre-crosslinked with 0.5% CaSO₄ which is known as the gel-point. Because of high cross-linking rate, A_6C_2 pre-crosslinked with 0.5% CaCl₂ and 0.5% CaSO₄ did not show any gel-point within the considered shear rate. When shear strain exceeded the intersection point (which is called the flow point), liquid-like phase started dominating solid-like phase and caused the material to flow. This flow stress value is helpful to understand the relationship between extrusion pressure and material flow. Applied pressure must exceed this LVR strain rate to successfully flow the material through the nozzle. The continuous drop of G' after the LVR indicates a gradual breakdown of the internal bonds for all the compositions.

4. Geometric analysis and full-scale scaffold fabrication

Acellular bi-layer scaffolds having dimension of $20\text{mm} \times 20$ mm were fabricated with the compositions of A_8C_0 , A_6C_2 , A_4C_4 , A_2C_6 , and A_0C_8 pre-crosslinked with $CaCl_2$ and $CaSO_4$ for inspecting their manufacturability or printability as shown in Figure 4.

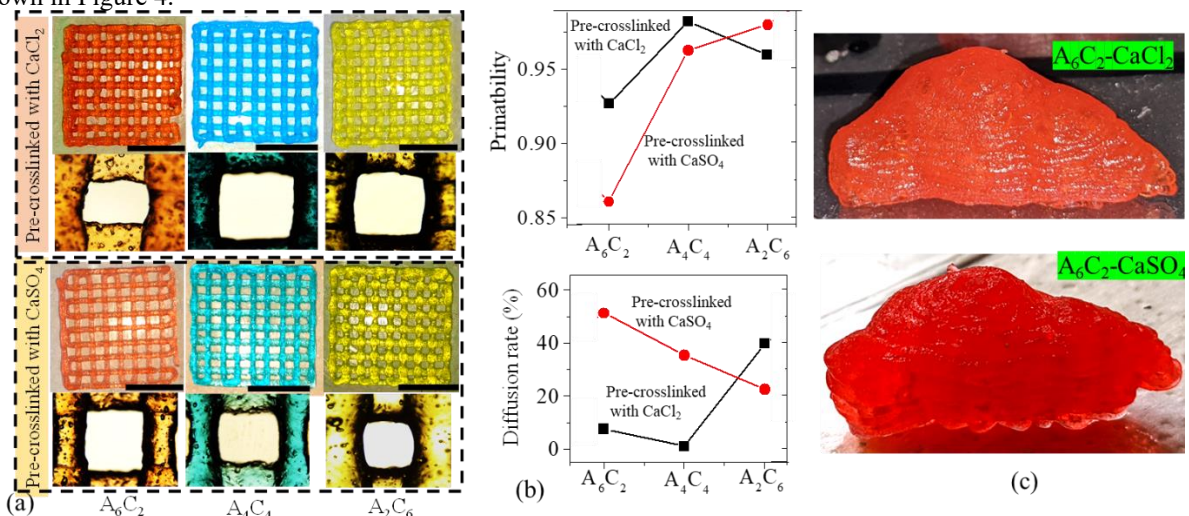


Figure 4: (a) Bi-layer scaffolds, (b) Probability and diffusion rate, and (c) Large scale freeform scaffolds fabricated with the compositions of A_6C_2 , A_4C_4 , and A_2C_6 compositions pre-crosslinked with 0.5% caso₄ and cacl₂. The length of black bar is 10 mm.

Even various compositions showed various amount of pore closure or diffusion rate, all of them showed a decent amount of printability having a range of 0.86-1.01 as shown in Figure 4(a). All the scaffolds fabricated with CaSO₄ pre-crosslinked compositions were extruded using 29 psi air pressure. Since, the yield stresses of those compositions were decreasing with increasing the weight percent of alginate, the pore size of the scaffolds fabricated with A_6C_2 , A_4C_4 , and A_2C_6 compositions were getting reduced. Eventually, the diffusion rate followed an increasing trend from 11% to 51% as shown in Figure 4(b). In case of compositions A_6C_2 pre-crosslinked with CaCl₂, we needed to increase the air pressure up to 45 psi to surpass the yield point and create flow of those compositions. This resulted uncontrolled extrusion, more material release, and eventually more diffusion rate (56% and 39% respectively) as shown in Figure 4(b). To demonstrate the capability of fabricating full-size scaffold, as a candidate composition, we chose A_6C_2 pre-crosslinked with CaCl₂ and CaSO₄, because of its good printability (0.96 and 0.98 respectively). A freeform liver model with a bounding box dimension and volume of $3.7 \times 1 \times 1.7$ (cm³) was used to fabricate as shown in Figure 4(c). No support structure was used to fabricate this scaffold which indicates the capability to fabricate full-scale freeform scaffold without sacrificing its geometric fidelity.

5. Discussion

A set of hybrid hydrogels such as A₆C₂, A₄C₄, and A₂C₆ was pre-crosslinked with 0.5% CaCl₂ and 0.5% CaSO₄. All pre-crosslinked hydrogels showed shear thinning behavior i.e., storage and loss modulus reduced with increasing the shear strain rate. Flow analysis showed that yield stress was percentage of alginate dependent. For same combination of alginate-CMC, higher yield and flow stresses were resulted pre-crosslinked with CaCl₂. Therefore, A₆C₂ pre-crosslinked with 0.5% CaCl₂ showed the highest yield stress. However, we did not get any flow point and corresponding flow stress within the considered limit of shear strain (0.01 to 100%). We could identify the flow point by increasing shear strain limit (> 100%). High yield stress requires greater applied force to surpass LVR region and make a smooth flow of material through the nozzle. It is well established that high applied pressure generates more shear stress and high cell death as a consequence [37]. Therefore, we can assume pre-crosslinked A₆C₂ will highly

affect the encapsulated cell where A_2C_6 will do minimally after extruding. However, we will choose compositions prepared with a certain portion of alginate for 3D bio-printing that it can help quick post-crosslinking and more reliable scaffold geometry during incubation period. The comparative study of the cell viability encapsulated in all precrosslinked compositions is a future direction of this research.

Analysis on bilayer 3D printed scaffolds revealed a good printability and shape holding capability of all precrosslinked compositions. However, A_6C_2 pre-crosslinked with $CaCl_2$ required a substantial amount of applied pressure where same compositions pre-crosslinked with $CaSO_4$ required 35% less applied pressure. Therefore, to fabricate a full scaffold ensuring good geometric fidelity and cell viability, compositions pre-crosslinked with $CaSO_4$ can be good candidates. We considered composition A_6C_2 pre-crosslinked with both 0.5% $CaCl_2$ and 0.5% $CaSO_4$ respectively to fabricate a large structure without any support structure where we found morphologically a minimal geometric difference between them. In future, we will use all the compositions to fabricate the same sample and find out the geometric difference among them.

6. Conclusion

Pre-crosslinked hydrogels with viscosity enhancer demonstrated an intriguing alternative for 3D bioprinting material for full-scale scaffold fabrication in this paper. From the applied pressure stand point, to fabricate a full-scaffold ensuring good geometric fidelity and cell viability, compositions pre-crosslinked with CaSO₄ can be good candidates. We believe, this pre-crosslinking-based physical and mechanical properties controlling technique can open a new avenue for 3D bio-fabrication of scaffold ensuring proper geometry.

Acknowledgements

Research was supported by New Hampshire-EPSCoR through BioMade Award #1757371 from National Science Foundation and New Hampshire-INBRE through an Institutional Development Award (IDeA), P20GM103506, from the National Institute of General Medical Sciences of the NIH.

References

- 1. Murphy, S.V. and A. Atala, *3D bioprinting of tissues and organs*. Nature biotechnology, 2014. **32**(8): p. 773-785.
- 2. Zeng, X., et al., *Printability improvement of rice starch gel via catechin and procyanidin in hot extrusion 3D printing.* Food Hydrocolloids, 2021: p. 106997.
- 3. Ozbolat, I.T. and M. Hospodiuk, *Current advances and future perspectives in extrusion-based bioprinting*. Biomaterials, 2016. **76**: p. 321-343.
- 4. Paxton, N.C., et al., Proposal to Assess Printability of Bioinks for Extrusion-Based Bioprinting and Evaluation of Rheological Properties Governing Bioprintability. Biofabrication, 2017.
- 5. Li, X., et al., Inkiet bioprinting of biomaterials. Chemical Reviews, 2020. 120(19): p. 10793-10833.
- 6. Wu, D. and C. Xu, *Predictive modeling of droplet formation processes in inkjet-based bioprinting*. Journal of Manufacturing Science and Engineering, 2018. **140**(10).
- 7. Wang, Z., et al., An ultrafast hydrogel photocrosslinking method for direct laser bioprinting. RSC Advances, 2016. **6**(25): p. 21099-21104.
- 8. Koch, L., et al., *Laser printing of skin cells and human stem cells*. Tissue Engineering Part C: Methods, 2009. **16**(5): p. 847-854.
- 9. Peltola, S.M., et al., *A review of rapid prototyping techniques for tissue engineering purposes*. Annals of medicine, 2008. **40**(4): p. 268-280.
- 10. Khoda, A., I.T. Ozbolat, and B. Koc, *A functionally gradient variational porosity architecture for hollowed scaffolds fabrication*. Biofabrication, 2011. **3**(3): p. 034106.
- 11. Malda, J., et al., 25th anniversary article: engineering hydrogels for biofabrication. Advanced materials, 2013. **25**(36): p. 5011-5028.
- 12. Unagolla, J.M. and A.C. Jayasuriya, *Hydrogel-based 3D bioprinting: A comprehensive review on cell-laden hydrogels, bioink formulations, and future perspectives.* Applied materials today, 2020. **18**: p. 100479.
- 13. Sánchez, E.M., et al., *Hydrogels for bioprinting: a systematic review of hydrogels synthesis, bioprinting parameters, and bioprinted structures behavior.* Frontiers in Bioengineering and Biotechnology, 2020. **8**.
- 14. Kirchmajer, D.M. and R. Gorkin Iii, *An overview of the suitability of hydrogel-forming polymers for extrusion-based 3D-printing*. Journal of Materials Chemistry B, 2015. **3**(20): p. 4105-4117.
- 15. Chen, Y., et al., 3D Bioprinting of shear-thinning hybrid bioinks with excellent bioactivity derived from gellan/alginate and thixotropic magnesium phosphate-based gels. Journal of Materials Chemistry B, 2020.

- 16. Yu, F., et al., *Evaluation of a polyvinyl alcohol-alginate based hydrogel for precise 3D bioprinting.* Journal of Biomedical Materials Research Part A, 2018. **106**(11): p. 2944-2954.
- 17. M'barki, A., L. Bocquet, and A. Stevenson, *Linking Rheology and Printability for Dense and Strong Ceramics by Direct Ink Writing*. Scientific Reports, 2017. 7(1): p. 6017.
- 18. Ahlfeld, T., et al., A methylcellulose hydrogel as support for 3D plotting of complex shaped calcium phosphate scaffolds. Gels, 2018. 4(3): p. 68.
- 19. Jin, Y., et al., Self-Supporting Nanoclay as Internal Scaffold Material for Direct Printing of Soft Hydrogel Composite Structures in Air. ACS Applied Materials & Interfaces, 2017. 9(20): p. 17456-17465.
- 20. Li, H., et al., 3D bioprinting of highly thixotropic alginate/methylcellulose hydrogel with strong interface bonding. ACS applied materials & interfaces, 2017. 9(23): p. 20086-20097.
- 21. Ahn, G., et al., Precise stacking of decellularized extracellular matrix based 3D cell-laden constructs by a 3D cell printing system equipped with heating modules. Scientific Reports, 2017. 7(1): p. 8624.
- 22. Di Giuseppe, M., et al., *Mechanical behaviour of alginate-gelatin hydrogels for 3D bioprinting*. Journal of the mechanical behavior of biomedical materials, 2018. **79**: p. 150-157.
- 23. Mouser, V.H., et al., *Yield stress determines bioprintability of hydrogels based on gelatin-methacryloyl and gellan gum for cartilage bioprinting.* Biofabrication, 2016. **8**(3): p. 035003.
- 24. Tabriz, A.G., et al., *Three-dimensional bioprinting of complex cell laden alginate hydrogel structures*. Biofabrication, 2015. 7(4): p. 045012.
- 25. Kuo, C., et al., *Printability of Hydrogel Composites Using Extrusion-Based 3D Printing and Post-Processing with Calcium Chloride.* J Food Sci Nutr, 2019. **5**: p. 051.
- 26. Ruther, F., et al., *Biofabrication of vessel-like structures with alginate di-aldehyde—gelatin (ADA-GEL) bioink.* Journal of Materials Science: Materials in Medicine, 2019. **30**(1): p. 1-14.
- 27. Kiyotake, E.A., et al., *Development and quantitative characterization of the precursor rheology of hyaluronic acid hydrogels for bioprinting.* Acta biomaterialia, 2019.
- 28. Gao, T., et al., *Optimization of gelatin–alginate composite bioink printability using rheological parameters: a systematic approach.* Biofabrication, 2018. **10**(3): p. 034106.
- 29. Rasheed, A., et al., Extrusion-Based Bioprinting of Multilayered Nanocellulose Constructs for Cell Cultivation Using In Situ Freezing and Preprint CaCl2 Cross-Linking. ACS omega, 2020. 6(1): p. 569-578.
- 30. Sarker, M., et al., Influence of ionic crosslinkers (Ca2+/Ba2+/Zn2+) on the mechanical and biological properties of 3D Bioplotted Hydrogel Scaffolds. Journal of Biomaterials science, Polymer edition, 2018. **29**(10): p. 1126-1154.
- 31. Rastin, H., et al., 3D bioprinting of a cell-laden antibacterial polysaccharide hydrogel composite. Carbohydrate Polymers, 2021. **264**: p. 117989.
- 32. Xu, D., et al., *PEDOT: PSS hydrogel film for supercapacitors via AlCl3-induced cross-linking and subsequent organic solvent treatments.* Materials Today Communications, 2020. **24**: p. 101090.
- 33. Freeman, F.E. and D.J. Kelly, *Tuning alginate bioink stiffness and composition for controlled growth factor delivery and to spatially direct MSC fate within bioprinted tissues.* Scientific reports, 2017. 7(1): p. 1-12.
- 34. Gonzalez-Fernandez, T., et al., *Alginate-based bioinks for 3D bioprinting and fabrication of anatomically accurate bone grafts.* Tissue Engineering Part A, 2021.
- 35. Han, Y. and L. Wang, *Sodium alginate/carboxymethyl cellulose films containing pyrogallic acid: physical and antibacterial properties.* Journal of the Science of Food and Agriculture, 2017. **97**(4): p. 1295-1301.
- Ouyang, L., et al., Effect of bioink properties on printability and cell viability for 3D bioplotting of embryonic stem cells. Biofabrication, 2016. **8**(3): p. 035020.
- 37. Habib, M.A. and B. Khoda. *A Rheological Study of Bio-Ink: Shear Stress and Cell Viability*. in *International Manufacturing Science and Engineering Conference*. 2021. American Society of Mechanical Engineers.